JACS Au
AN OPEN ACCESS JOURNAL OF THE AMERICAN CHEMICAL SOCIETY

pubs.acs.org/jacsau
Article

Synthetic Cation Transporters Eradicate Drug-Resistant *Staphylococcus aureus*, Persisters, and Biofilms

Pak-Ming Fong, Victor Yat-Man Tang, Lu Xu, Bill Hin-Cheung Yam, Halebeedu Prakash Pradeep, Yuhui Feng, Liang Tao, Richard Yi-Tsun Kao,* and Dan Yang*

Cite This: *JACS Au* 2025, 5, 1328–1339
Read Online

ACCESS | Metrics & More | Article Recommendations | Supporting Information

ABSTRACT: New drugs are urgently required to address the ongoing health crisis caused by methicillin-resistant *Staphylococcus aureus* (MRSA) infections. Added to the challenge is the difficult-to-treat persister cells and biofilm which are tolerant to the antibiotics. Here we report a new approach to these problems, describing the design and synthesis of aminoxy-acid–based dipeptides that facilitate cation transport across cell membranes to disrupt bacterial ion homeostasis. Remarkably, these synthetic cation transporters display significant antibacterial activity against MRSA, while maintaining high selectivity over mammalian cells. They also effectively eliminate bacterial persisters and reduce established biofilms. Additionally, they inhibit biofilm formation and suppress bacterial virulent protein secretion, even at subinhibitory concentrations. Their associated antibiotic effects support their in vivo efficacy in murine skin and bloodstream MRSA infection models with no observable toxicity to the host. Mode-of-action analysis indicates that these cation transporters induce cytoplasmic acidification, hyperpolarization, and calcium influx, accelerating autolysis. Given their potent activity against bacterial persisters and biofilms, synthetic cation transporters are an emergent and promising class of compounds in the fight against MRSA infections.

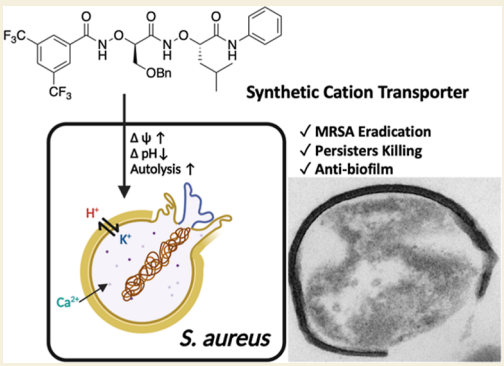

KEYWORDS: *antibiotics, ion transport, structure activity relationships, persister, biofilm*

INTRODUCTION

The escalating global health crisis associated with MDR bacterial strains accounts for an estimated 4,850,000 deaths annually.[1] MRSA is one of the most concerning MDR bacterial strains with global prevalence, causing severe infections such as bacteremia, sepsis, endocarditis, and osteomyelitis.[2−4] Beyond its antibiotic resistance, *Staphylococcus aureus* forms dormant phenotypic variants called persisters, which are highly tolerant to antibiotic treatment.[5] These persisters also contribute to forming a bacterial polymeric network known as biofilm, wherein the bacteria are shielded from antibiotics by a protective extracellular matrix.[6] The lack of antibiotics with new modes of action further exacerbates the challenge of MRSA treatment.[7]

Bacteria have developed sophisticated mechanisms to regulate ion homeostasis, which is crucial for osmoregulation and maintaining the proton motive force (PMF).[8] Disrupting ion homeostasis is lethal to bacteria, as evidenced by the strong antibacterial effect of natural ionophores.[9] Although these ionophores are commonly used in agriculture,[10] they can exhibit toxicity to some animals.[11] Synthetic ion transporters have also been developed to inhibit bacterial growth; however, they often lack sufficient selectivity for bacterial versus mammalian cells, and their precise mechanism remains underexplored.[12,13] Together with the challenge to eliminate bacterial persisters and biofilms, this makes the development of such molecules, especially those with low mammalian cell toxicity, both challenging and imperative.

Our recent studies have demonstrated that synthetic cation transporters **1** and **2**, built on α-aminoxy acid scaffolds, exhibit low cytotoxicity toward typical eukaryotes while selectively eliminating nonadherent cancer stem cells (CSCs).[14] This selectivity stems from exploiting the subcellular pH gradients and hyperpolarized mitochondrial membranes of CSCs. Given the similar membrane potential and pH gradient contributing to the PMF in bacteria,[15] we hypothesized that these synthetic cation transporters could serve as selective antibacterial agents.

RESULTS AND DISCUSSION

Design, Synthesis, and Antibacterial Profile of Synthetic Cation Transporters

The antibacterial activity of compounds **1** and **2** on MRSA Mu3 was evaluated to test our hypothesis. Their minimum inhibitory

Received: December 9, 2024
Revised: February 5, 2025
Accepted: February 6, 2025
Published: February 14, 2025

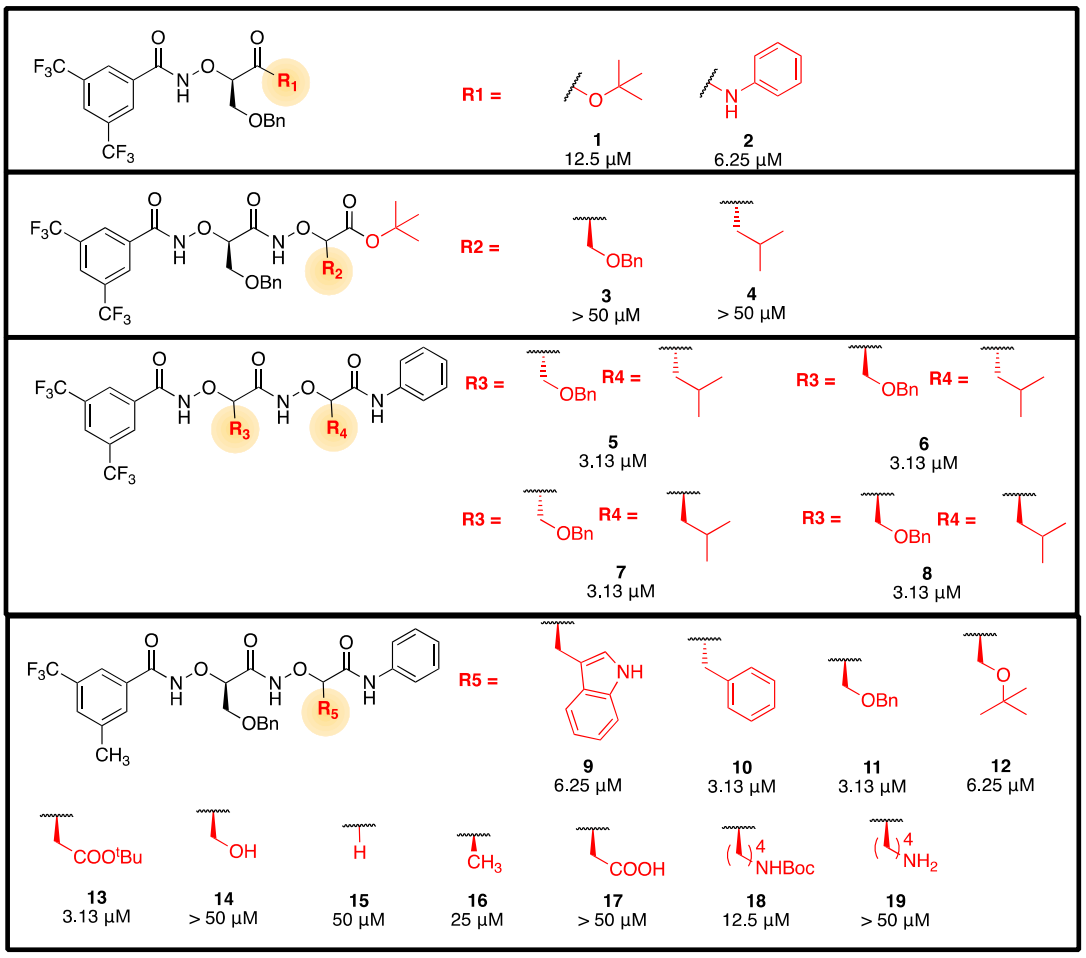

Figure 1. Structure−activity relationship of compounds **1**−**19**. Chemical structures of compounds **1**−**19** and their MIC (μM) on MRSA Mu3.

concentration (MIC) values were found to be 12.5 and 6.25 μM, respectively. We hypothesized that increased hydrophobicity might enhance membrane penetration, thereby improving antibacterial efficacy. Prior studies indicated that hydrophobic compounds with log P above six did not cause significant mitochondrial toxicity, as they accumulated in the cytoplasmic membrane instead of the mitochondrial membrane.[16] Consequently, we designed and synthesized 17 aminoxy dipeptides with varying hydrophobicity and evaluated their antibacterial activities (Figure 1). Analogs featuring an anilide group at the C-terminus (compounds **5**−**19**) demonstrated antibacterial activities, which positively correlated with hydrophobicity (Figure S1). In contrast, compounds **3** and **4**, containing a *tert*-butyl ester group in the C-terminus, did not show a significant inhibitory effect. Additionally, altering the chirality of aminoxy acids (compounds **5**−**8**) did not impact their antibacterial potency, suggesting that these dipeptides do not interact with specific protein targets. Compound **6** with a stronger antibacterial activity (MIC 3.13 μM against MRSA) was chosen for further study. It was highly effective against Gram-positive bacteria but not Gram-negative bacteria except *Escherichia coli* mutants NR698[17] and RAM127[18] with a defective outer membrane barrier (Table S1). This suggests that the outer membrane of Gram-negative bacteria restricts the entry of compound **6**. Compound **6** was bactericidal against MRSA (Figure S2), outperforming the last-resort antibiotics like vancomycin and daptomycin in eliminating late exponential phase populations (Figure 2b). In addition to its bactericidal properties, compound **6** also attenuated the hemolytic ability of *S. aureus* (Figure S3). Secretome analysis (Figure S4) revealed that compound **6** suppressed the secretion of multiple virulent proteins even at subinhibitory concentration, which could prevent *S. aureus* infection in the host.[19] Notable virulent proteins that were significantly repressed include hemolysins Hld and Hly, pro-inflammatory phenol-soluble modulins Psmα1 and Psmβ2, pore-forming leucotoxins LukDv and LukEv, and the immunoglobulin-binding protein Sbi.[20]

We further explored the antibacterial effect of compound **6** on *S. aureus* persisters, which are tolerant to most conventional antibiotics.[21] While persisters were completely tolerant to 6 classes of conventional antibiotics we tested, compound **6** completely eradicated these enriched persisters (Figure 2c). Additionally, we tested the antibacterial activity of compound **6** on *S. aureus* biofilms, which are mainly composed of persisters by crystal violet staining.[22] Vancomycin only demonstrated limited antibiofilm activity even at its 128-fold MIC. In contrast, these difficult-to-treat biofilms could be efficiently reduced by compound **6** (Figure 2d). The biofilm was also stained with SYTO9 and PI, which visualized the living and dead bacteria, respectively. After the treatment of compound **6**, the live-to-dead ratio of biofilm intensity and biovolume is significantly lower than DMSO-treated biofilm (Figure S5a,b). Furthermore, compound **6** could effectively suppress *S. aureus* biofilm production even at subinhibitory concentrations as low as 49 nM (1/64 of its MIC) (Figure 2e). These results motivated us to

https://doi.org/10.1021/jacsau.4c01198
JACS Au 2025, 5, 1328−1339

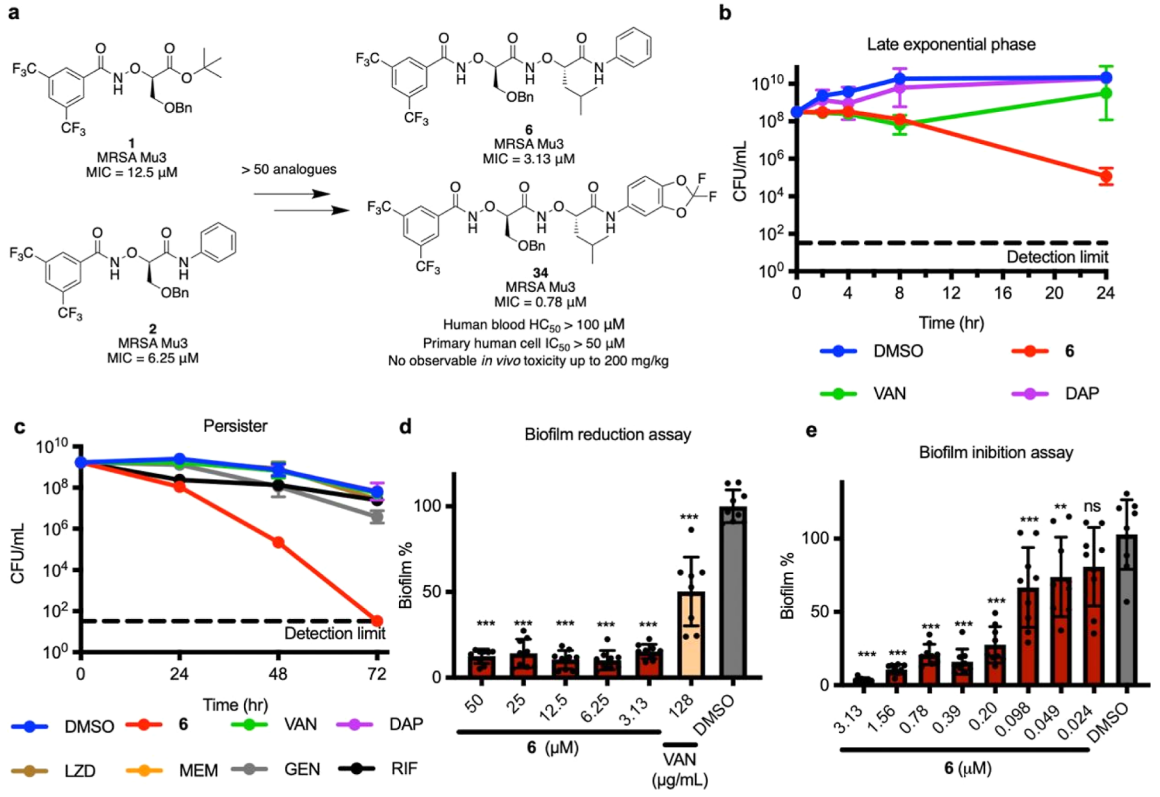

Figure 2. Antibacterial profile of compound **6** (a) chemical structure and MIC of compound **6** and **34**. (b) Time-dependent killing on late exponential phase MRSA Mu3 by with 10 × MIC of different compounds: compound **6** (31.25 μM), vancomycin (VAN) (10 μg/mL), daptomycin (DAP) (10 μg/mL) or 1% DMSO. (c) Persister assay. *S. aureus* ATCC29213 persisters were challenged with 10 × MIC of different compounds: compound **6** (31.25 μM), rifampin (RIF) (0.078 μg/mL), linezolid (LZD) (40 μg/mL), meropenem (MEM) (2.5 μg/mL), daptomycin (DAP) (10 μg/mL), vancomycin (VAN) (10 μg/mL), gentamicin (GEN) (5 μg/mL) or 1% DMSO. (d) Biofilm reduction assay. 24 h pre-established *S. aureus* ATCC35556 biofilm was treated with compound **6**, 128 × MIC vancomycin or 1% DMSO. (e) Biofilm inhibition assay. *S. aureus* ATCC35556 was treated with compound **6** or 1% DMSO (negative control) for 24 h. Biofilm was then quantified.

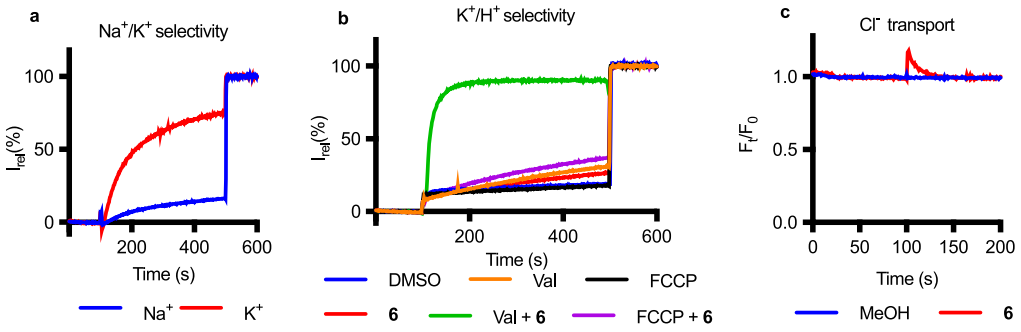

Figure 3. Compound **6** transported H^+ (fastest) > K^+ > Na^+ > Cl^- (slowest) in the liposome model. (a,b) In HPTS assay, (a) Na^+/K^+ transport selectivity of compound **6** (12.5 μM) and (b) ion transport activity of compound **6** (195 nM) with or without potassium transporter valinoymcin (25 nM) or protonophore FCCP (100 nM) were monitored. (c) In SPQ assay, Cl^- transport activity of compound **6** (100 μM) was monitored. The experiments were repeated at least in duplicate and representative results were displayed.

investigate the antibacterial mechanism underlying the efficacy of compound **6**.

Dissipation of PMF by Synthetic Cation Transporter 6

We first evaluated the ion transport activity of compound **6** in large unilamellar vesicles (LUVs) encapsulating the pH-sensitive probe 8-hydroxypyrene-1,3,6-trisulfonic acid (HPTS).[23] Compound **6** showed a faster potassium transport (EC_{50} = 0.67 μM) than sodium (EC_{50} = 15.40 μM) (Figures 3a,S6a,b and S7). To understand the role of protons in potassium transport, we added the potassium transporter valinomycin (Val) or protonophore carbonyl cyanide-4-(trifluoromethoxy)phenylhydrazone (FCCP) alongside compound **6** to compensate for any potential rate-limiting factors.[24] Adding valinomycin but not FCCP resulted in a significant increase in HPTS fluorescence but no increase was observed with FCCP (Figure 3b). This suggests compound **6** is an electrogenic transporter that transports protons more rapidly than potassium. To assess anion transport activity, we used LUVs encapsulating 6-methoxy-*N*-(3-sulfopropyl)quinolinium (SPQ),[25] whose fluorescence can be quenched by chloride. Upon adding compound **6**, no fluorescence quenching was

https://doi.org/10.1021/jacsau.4c01198
JACS Au 2025, 5, 1328−1339

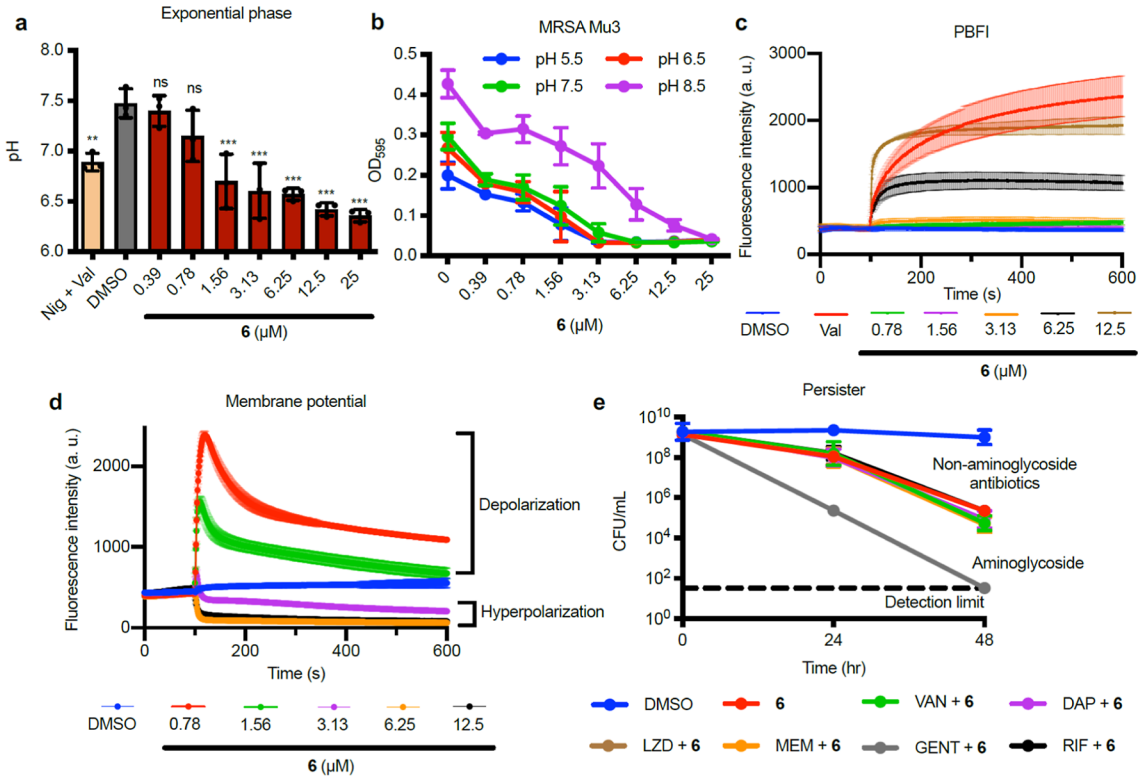

Figure 4. Compound **6** dissipates *S. aureus* PMF. (a) pH of exponential phase *S. aureus* upon addition of compound **6**, positive controls nigericin (Nig) (2 μM) with valinomycin (Val) (2 μM) and negative control 1% DMSO. (b) MICs of compound **6** against MRSA Mu3 at different pH. (c) *S. aureus* intracellular potassium ion leakage upon the addition of compound **6** and positive control valinomycin. (d) The inhibitory concentration of compound **6** induced MRSA Mu3 hyperpolarization. (e) The synergy of gentamicin and compound **6** against *S. aureus* persister. *S. aureus* persister cells were challenged with compound **6** (31.25 μM) or combined with different antibiotics: rifampin (RIF) (0.078 μg/mL), linezolid (LZD) (40 μg/mL), meropenem (MEM) (2.5 μg/mL), daptomycin (DAP) (10 μg/mL), vancomycin (VAN) (10 μg/mL), gentamicin (GEN) (5 μg/mL).

observed, which indicates that compound **6** does not transport chloride (Figure 3c).

This led us to elucidate whether compound **6** can promote ion transport in *S. aureus*. In Gram-positive bacteria, electron transport chains extrude protons into the periplasmic space to generate the proton motive force (PMF) necessary for ATP synthesis.[26] The PMF comprises electric potential ($\Delta\psi$) and proton gradient (ΔpH). Considering that compound **6** could transport protons in the liposome model, we explored whether compound **6** could balance ΔpH in bacteria, leading to cytoplasmic acidification. We used a ratiometric pH-sensitive GFP reporter[27] to monitor *S. aureus* cytoplasmic pH (Figure S8). The addition of compound **6** resulted in a significant pH drop in both exponential and stationary phase *S. aureus* (Figures 4a and S9), suggesting cytoplasmic acidification. Furthermore, compound **6** showed a stronger antibacterial effect in an acidic environment compared to a basic environment (Figures 4b and S10a). This trend did not appear in other antibiotics such as gentamicin (Figure S10b,c).[28] These observations further support the critical role of pH homeostasis disruption in the antibacterial mechanism of compound **6**. We then monitored extracellular potassium content using the cell-impermeable potassium-sensitive fluorescent probe PBFI.[29] We observed a sharp increase in fluorescence upon the addition of compound **6**, indicating potassium efflux from bacteria (Figure 4c). Inductively coupled plasma mass spectrometry (ICP−MS) also confirmed a reduction in cytoplasmic potassium content after treatment of compound **6** (Figure S11a). In contrast, compound **6** did not significantly alter cytoplasmic potassium content in the Gram-negative bacterium *E. coli*, which is resistant to compound **6** (Figure S11b). These findings collectively indicate compound **6** functions as an H^+/K^+ antiporter in *S. aureus*.

Since membrane potential arises from the ion concentration gradient across the membrane, compound **6** may alter it by disrupting bacterial ion homeostasis. Hence, we used 3,3′-dipropylthiacarbocyanine iodide ($DiSC_3(5)$) to monitor possible changes in membrane potential.[30] An increase in ($DiSC_3(5)$) fluorescence was observed after the addition of compound **6** at a subinhibitory concentration (<3.13 μM), indicating membrane depolarization (Figures S12 and 3d). This observation corroborates our experimental result in the liposome model since compound **6** could lead to faster proton influx than potassium efflux. However, we observed fluorescence quenching when compound **6** was added at an inhibitory concentration (≥3.13 μM) (Figure 4d), likely due to bacteria's tight control of $\Delta\psi$ and ΔpH. When one component dissipates, the other compensates to maintain a constant PMF.[30] At an inhibitory concentration of compound **6** that significantly reduced *S. aureus* ΔpH via proton influx, the PMF could be restored by enhancing $\Delta\psi$ (i.e., hyperpolarization). Furthermore, bacterial membrane hyperpolarization was known to increase aminoglycoside uptake and thus facilitate the eradication of bacterial persisters.[31] Consistent with this, we observed that compound **6** accelerated the bactericidal activity of aminoglycosides against *S. aureus* persisters (Figure 4e).

https://doi.org/10.1021/jacsau.4c01198
JACS Au 2025, 5, 1328−1339

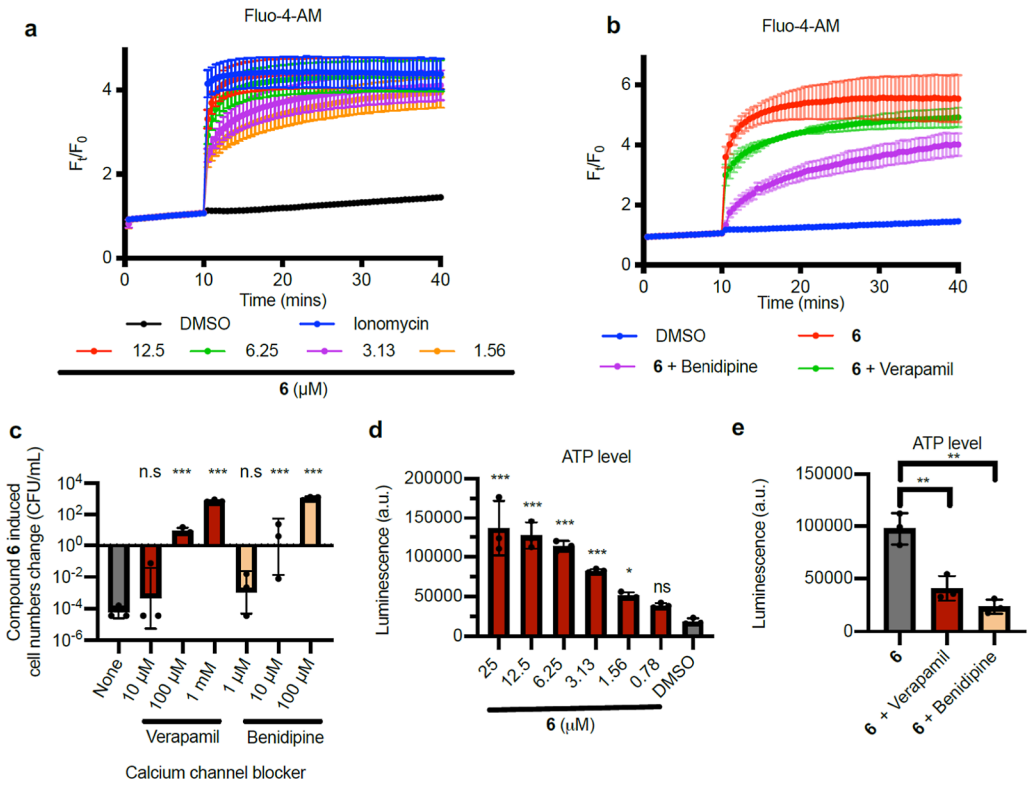

Figure 5. Compound **6** induced calcium influx in *S. aureus*. (a) Induction of calcium influx into MRSA Mu3 by compound **6** and positive control ionomycin (1 μM). (b) Alleviation of calcium influx by calcium channel blocker verapamil (1 mM) or benidipine (100 μM). (c) Protection of bacteria from the bactericidal effect of compound **6** by calcium channel blockers verapamil and benidipine. (d) Elevation of cellular ATP after compound **6** treatment. MRSA Mu3 was treated with compound **6** for 10 min and ATP level was measured. (e) Alleviation of compound **6** induced-ATP level elevation by calcium channel blocker. MRSA Mu3 was treated with compound **6** or in combination with verapamil (1 mM) or benidipine (100 μM) for 10 min and ATP level was measured.

Synthetic Cation Transporter 6 Induced Calcium Influx

In biological systems, activating a specific ion channel can change membrane potential, which may subsequently activate or deactivate other ion channels.[32] A classic example of this is calcium homeostasis in eukaryotic cells. Calcium, as a crucial second messenger, controls essential physiological functions such as neurotransmitter release and muscle contraction, and even triggers apoptosis.[33−35] Studies on calcium signaling in prokaryotic systems are rare, although calcium has been shown to induce autolysis in *Streptococcus pneumoniae*.[36] Calcium homeostasis is precisely regulated by voltage-gated calcium channels. Hyperpolarization can activate these channels, increasing calcium influx.[37] Our previous work showed that synthetic ion channels could regulate voltage-gated calcium channels by altering membrane potential in mammalian cells.[38] Given that compound **6** induced hyperpolarization in *S. aureus*, we explored whether this compound could also trigger calcium influx by modulating membrane potential.

We used a calcium-sensitive fluorescence probe, Fluo-4-AM, to measure the intracellular calcium level in *S. aureus*. Compound **6** was found to immediately increase fluorescence in a concentration-dependent manner, indicating calcium influx in *S. aureus* (Figure 5a). ICP−MS also showed an increase in cytoplasmic calcium content in *S. aureus* (Figure S13a) but not *E. coli* (Figure S13b) after compound **6** treatment. The addition of verapamil (L-type calcium channel blocker)[39] or benidipine (triple L-, T-, and N-type calcium channel blocker)[40] reduced the fluorescence enhancement (Figure 5b), indicating that the activation of calcium channels was involved in the calcium influx triggered by compound **6**. Moreover, verapamil and benidipine rescued *S. aureus* from compound **6**-induced toxicity, suggesting that the overload of cytoplasmic calcium contributes to the compound's bactericidal activity (Figure 5c). Compound **6** also induced a dose-dependent ATP boost in *S. aureus* (Figure 5d), a phenomenon reported for mammalian cells where calcium influx could stimulate the mitochondrial oxidative phosphorylation to regulate cellular ATP homeostasis.[41,42] This ATP increase was attenuated by adding calcium channel blockers (Figure 5e), further supporting the role of calcium influx in this process. While the exact biological implication of the ATP increase in *S. aureus* is not fully understood, prior studies on *E. coli* suggested that excess ATP may be hydrolyzed by F_1F_0-ATPase in reverse direction, leading to hyperpolarization and cell death.[43]

Compound 6 Accelerated *S. aureus* Autolysis

To understand the downstream effect of the ion homeostasis disruption, we attempted to generate mutants resistant to compound **6**. We obtained mutants with MICs higher than 100 μM by continuously reinoculating *S. aureus* into a subinhibitory concentration of compound **6** (Table S2 and Figure S14). Notably, these mutants did not show cross-resistance to any conventional antibiotics tested (Table S3), indicating that resistance mechanisms developed were specific to compound **6** without conferring broad-spectrum resistance to other antibiotics. Interestingly, some mutants had significantly weaker hemolytic abilities than the wild type (Figure S15), suggesting an evolutionary trade-off where the bacteria compromise their virulence in exchange for survival in the presence of compound **6**, highlighting a potential survival cost associated with

https://doi.org/10.1021/jacsau.4c01198
JACS Au 2025, 5, 1328−1339

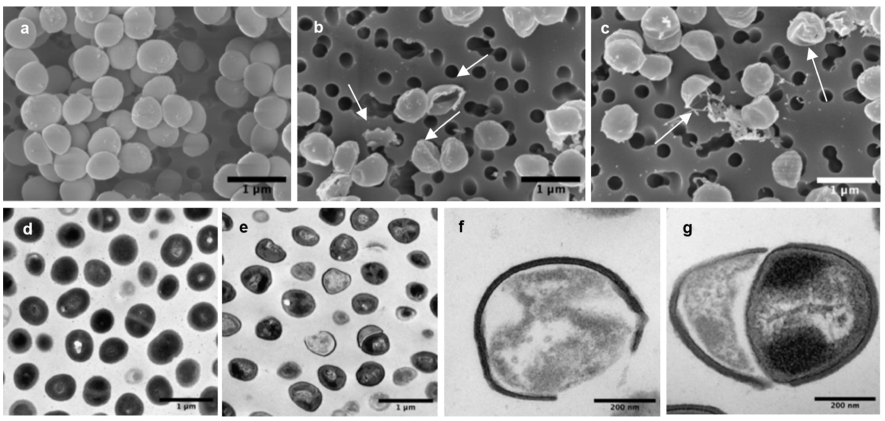

Figure 6. FESEM and TEM images of *S. aureus* ATCC29213. (a–c) FESEM images of *S. aureus* ATCC29213 treated with (a) DMSO or (b,c) compound **6** (12.5 μM). Arrowheads point to damaged *S. aureus*. (d–g) TEM images of *S. aureus* ATCC29213 treated with (d) DMSO or (e–g) compound **6** (12.5 μM).

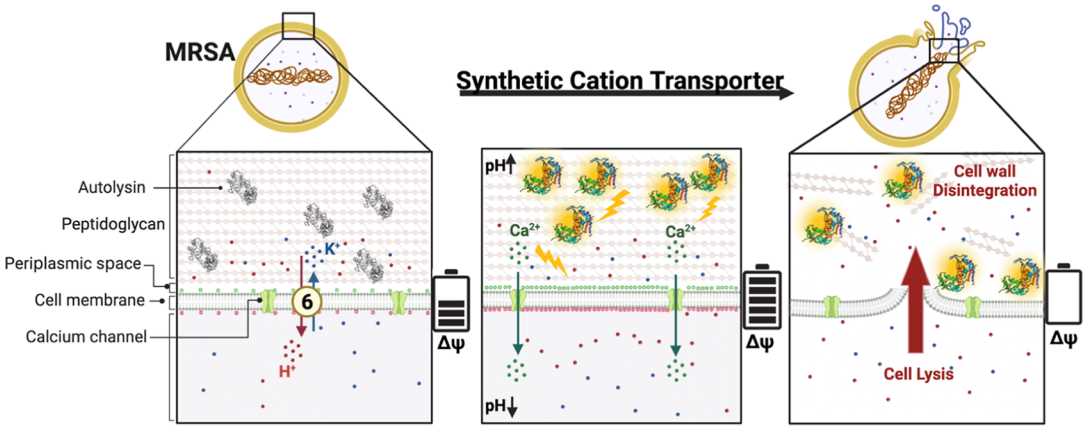

Figure 7. Proposed antibacterial mechanism of cation transporter compound **6**. (a) Compound **6** mediates H^+/K^+ antiport, with much faster H^+ transport than K^+, across the cell membrane of *S. aureus*. (b) The ΔpH across the cell membrane decreases. The cell membrane undergoes hyperpolarization, followed by calcium influx. Autolysins are activated. (c) Autolysis is accelerated, leading to an osmotic cell burst.

developing resistance. It is important to note that any pathogens capable of causing infection in the presence of antibiotics should exhibit both resistance to antibiotics and virulence.[44]

Whole-genome sequencing of the highly resistant mutants revealed a frameshift in *SagB* and mutations in *WalR* (Table S2). SagB is a membrane-bound glucosaminidase that complexes with membrane protein SpdC to cleave the nascent peptidoglycan from the cell membrane. *SagB* knockout mutant drastically slows down *S. aureus* autolysis. Moreover, the inactivation of SagB–SpdC complexes is known to increase the resistance to lysostaphin, the glycyl–glycyl endopeptidase that hydrolyzes staphylococcal peptidoglycan by cleaving pentaglycine cross bridge.[45,46] WalR, on the other hand, is a response regulator of the essential two-component system WalRK. It controls the transcription of autolysins, bacterial hydrolases that cleave staphylococcal peptidoglycan to facilitate cell division.[47,48] Even a minor perturbation in the level of these autolysins could result in dysregulation of cell wall turnover.[49] These mutations likely contribute to compound **6** resistance altering the autolysis machinery of *S. aureus*.

Optical density is a well-established indicator for assessing autolysis, as it decreases when autolysis is accelerated.[36,50] Upon the treatment of compound **6**, the optical density of *S. aureus* decreased, indicating that the compound accelerates autolysis (Figure S16a). To link this observation to the bactericidal activity of compound **6**, we generated two markerless *Atl* and *sagB* knockout mutants. Atl is the primary peptidoglycan hydrolase in *S. aureus*. It is a bifunctional enzyme that yields both amidase and glucosaminidase after proteolytic cleavage.[51] Compound **6** showed statistically weaker bactericidal activity in both *Atl* and *SagB* knockout strains (Figure S17), which supports the bactericidal activity of compound **6** closely linked to the activity of autolysins. To further investigate the downstream effects of autolysis acceleration, we applied field emission scanning electron microscopy (FESEM) and transmission electron microscopy (TEM) to examine the morphology of *S. aureus* after the treatment with compound **6**. SEM and TEM micrographs of *S. aureus* treated with DMSO control showed the expected characteristic spherical shape (Figures 6a,d and S18a). In contrast, those treated with compound **6** revealed bacterial membrane rupture and lysis (Figures 6b,c and S18b) in SEM, irregular cell morphology, particularly lack of cell wall at the septum of dividing cells (Figure 6e–g) in TEM, which aligns with the literature on autolysin location.[52] Taken together, these observations strongly support our hypothesis that compound **6** triggers dysregulation of autolysis. This dysregulation leads to cell death, likely due to extensive autolysis followed by osmotic stress and membrane rupture.

https://doi.org/10.1021/jacsau.4c01198
JACS Au 2025, 5, 1328–1339

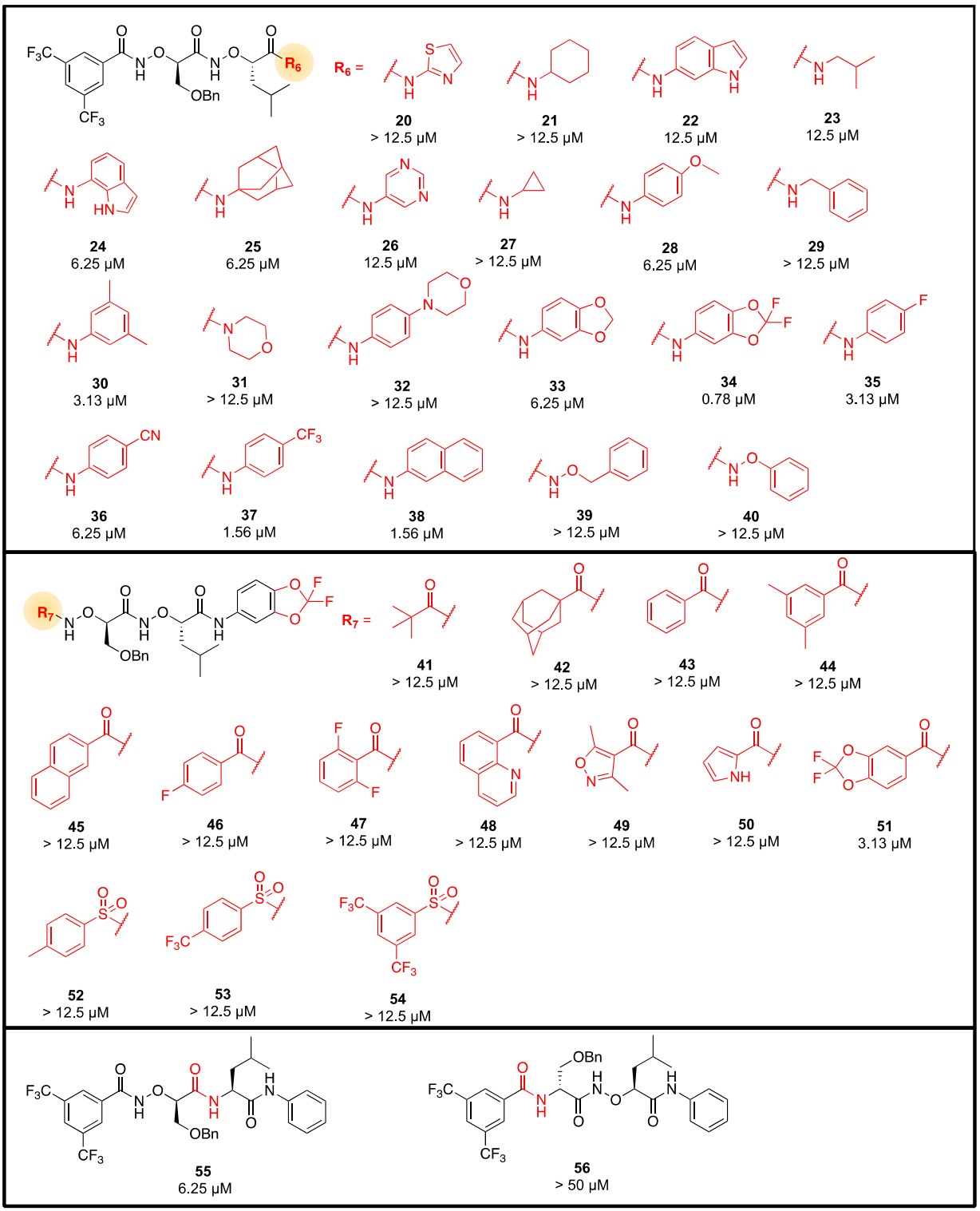

Figure 8. Structure−activity relationship of compounds **20**−**56**. Chemical structures of compounds **20**−**56** and their MIC (μM) on MRSA Mu3.

Under-Secretion of Autolysin upon Compound 6 Treatment

Next, we sought to understand the mechanism behind the observed acceleration of autolysis. Intriguingly, secretome analysis revealed that most peptidoglycan hydrolase domains containing proteins were under-secreted following treatment with compound **6** (Figure S19). Real-time RT-qPCR further confirmed reduced transcript levels of autolysins (Figure S20). These results demonstrated that the acceleration of autolysis was not due to the overexpression of autolysins. The reduction of autolysin expression may represent a bacterial defense system aimed at minimizing hydrolytic damage caused by compound **6** to the cell wall. This is like the observations with cell wall-targeting β-lactam antibiotics, where bacteria under-express autolysin to prevent excessive cell wall degradation.[53] Such a bacterial defense system has been previously described in *Bacillus subtilis*. When the autolysin activity becomes excessive,

https://doi.org/10.1021/jacsau.4c01198
JACS Au 2025, 5, 1328−1339

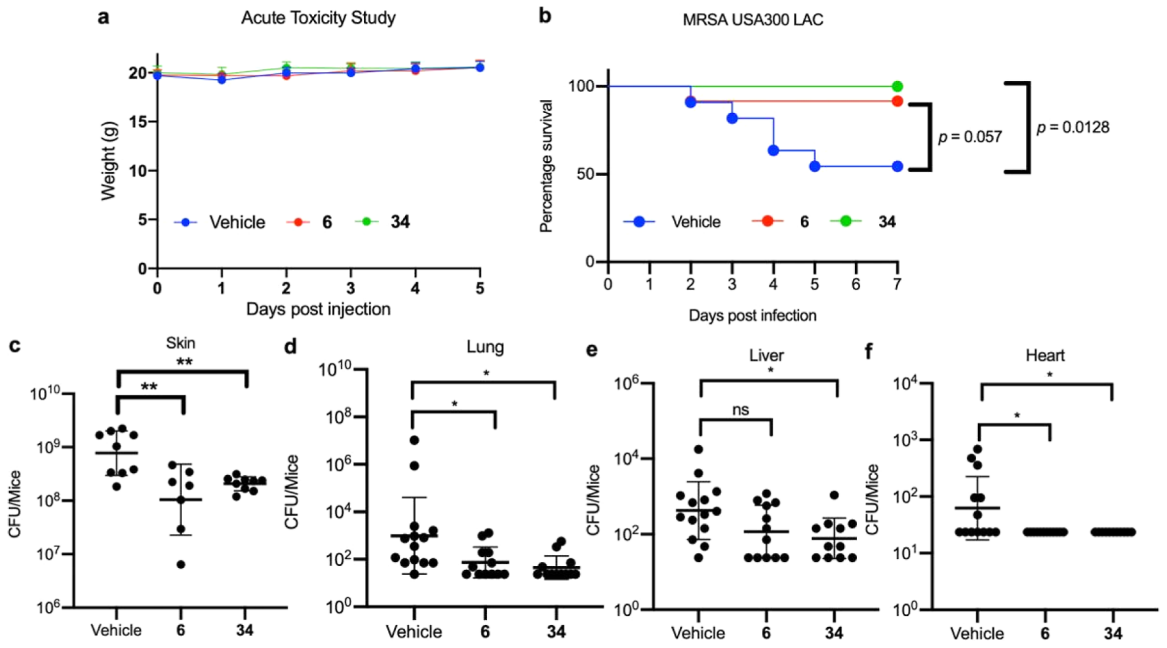

Figure 9. In vivo efficacy of compounds **6** and **34**. (a) Changes in mean body weight of mice treated with vehicle, compound **6** (200 mg/kg), or **34** (200 mg/kg) in the acute toxicity study. (b) Survival curves depicting the efficacy of compounds **6** (10 mg/kg/day) and **34** (10 mg/kg/day) in the lethal murine bloodstream infection model. (c) Bacterial load in the skin of MRSA USA300 LAC infected mice treated with **6** (20 mg/kg/day), **34** (20 mg/kg/day), or vehicle in a skin infection model. (d–f) Bacterial loads in the (d) lung, (e) liver, and (f) heart of MRSA USA300 LAC infected mice and treated with compound **6** (10 mg/kg/day), **34** (10 mg/kg/day) or vehicle in a bloodstream infection model.

the cell wall cleavage products inhibit WalRK signaling, suppressing the expression of WalR-dependent autolysins, and forming a feedback loop that maintains cell wall homeostasis.[49,54] In addition to transcriptional and translational regulation, autolysin activity is also subject to post-translational modulation.[55,56] In *B. subtilis*, studies have shown that the dissipation of PMF can affect autolysin activity, leading to cellular lysis.[57,58] Autolysin activities are also pH-dependent, with lower hydrolytic efficiencies observed in the periplasmic space due to a localized acidic environment.[59−61] A similar study in *S. aureus* suggested that dissipation of the pH gradient can activate autolysins in a wall-teichoic acid-dependent manner.[62] While we cannot exclude the possibility that other factors might also contribute to the overall mechanism, the evidence strongly suggests that compound **6**, which alters membrane potential, pH gradient, and ion composition across cell membranes, can activate autolysins and lead to dysregulated cellular autolysis and subsequent cell lysis (Figure 7). These findings highlight that post-translational regulation of autolysins is a key component in the mechanism of action of compound **6**, giving rise to dysregulated autolysis and cell death.

Further Structural Optimization of Compound 6 Yielded Compound 34 with Superior Antibacterial Activities

To further optimize the antibacterial properties, we conducted structural optimization of compound **6** by primarily modifying the C-terminus and N-terminus (Figure 8). We first synthesized 21 analogs with C-terminal alterations and determined their MICs. Our structure−activity relationship (SAR) analysis discovered that the C-terminal aromatic amide is essential for antibacterial activity, as its removal (such as *tert*-butyl esters **3** and **4**, aliphatic amides **21**, **27**, **29**, and **31**, as well as oxyamides **39** and **40**) led to reduced antibacterial efficacies. The hydrophobic isobutyl amide **23** and adamantanamide **25** displayed modest antibacterial activity with MIC values of 12.5 and 6.25 μM, respectively. For aromatic amide analogs, their hydrophobicity and antibacterial activity were positively correlated (Figure S21). Compound **34** (Figure 2a), featuring 2,2-difluoro-1,3-benzodioxole as the C-terminal substituent, exhibited the highest antibacterial activity (MIC = 0.78 μM). Then we synthesized 14 analogs with modified N-terminus while keeping 2,2-difluoro-1,3-benzodioxole as the C-terminal substituent. Only compound **51**, which possesses 2,2-difluoro-1,3-benzodioxole in its N-terminus, was antibacterial (MIC = 3.13 μM). This aligns with previous findings, suggesting that an electron-withdrawing group is required on the N-terminus substituent of aminoxy cation transporters. This increases the acidity of aminoxy amide NH to facilitate its deprotonation in the physiological environment.[14] NMR titration of compound **6** with tetrabutylammonium hydroxide (TBAOH) further confirmed that aminoxy amide NHs are more acidic than those of anilide amides (Figure S22). Replacement of the more acidic aminoxy amide with a less acidic ordinary amide (compounds **55** and **56**) resulted in a decrease in their antibacterial activities (Figure 8). These findings provide support for the notion that the acidic aminoxy amide NH undergoes deprotonation and reprotonation in the physiological environment, which is crucial for compound **6** to effectively eliminate *S. aureus* through proton influx. In addition, ICP−MS analysis did not detect any significant change in cytoplasmic calcium and potassium content after the addition of compound **56** (Figure S23). This evidence further strengthens the notion that the disruption of ion homeostasis contributes to the overall antibacterial mechanism of the cation transporter.

We proceeded to investigate the antibacterial properties of compound **34**, which exhibited the highest antibacterial activity among the tested compounds. Analogous to compound **6**, compound **34** demonstrated activity against a range of Gram-positive bacteria while showing limited activity against Gram-negative bacteria (Table S4). Furthermore, it displayed efficacy

https://doi.org/10.1021/jacsau.4c01198
JACS Au 2025, 5, 1328−1339

against early and late-exponential-phase MRSA, persister cells, and biofilm (Figure S24). Like compound **6**, compound **34** was found to alter *S. aureus* cytoplasmic potassium and calcium levels (Figures S11 and S13). Moreover, it reduced the optical density of *S. aureus* (Figure S16b) and induced abnormal cell morphology as observed in FESEM (Figure S18c−e) and TEM examinations (Figure S18f−h). Additionally, compound **34** exhibited weaker antibacterial activity against suppressor mutants of compound **6** compared to the sensitive strain (Table S5). These results strongly suggest that compounds **6** and **34** share a common antibacterial mechanism, characterized by the disruption of ion homeostasis and autolysin-mediated cell death in *S. aureus*.

Evaluation of the In Vivo Antibacterial Efficacy of Compounds 6 and 34

We further evaluated the therapeutic potential of compounds **6** and **34** by first testing their safety profile. The in vitro toxicities against mammalian cell lines were assessed using MTT assays. Despite the indiscriminate toxicity of previously reported cation transporters,[11−13] compounds **6** and **34** showed rather limited toxicity against a range of mammalian cell lines and primary human cells (Figures S25 and S26). Moreover, they did not exhibit any noticeable hemolytic activity (Figure S27). Most importantly, they showed no observable in vivo toxicity as evidenced by the lack of mortality in mice, stable body and tissue weights, normal histology of major organs, and unremarkable hematology and liver function profiles. These findings were consistent across both the acute toxicity study (up to 200 mg/kg) and the maximum tolerance study (up to 40 mg/kg/day) (Figures 9a, S28−S29, Tables S10−S17).

With this promising in vivo safety profile, we sought to evaluate in vivo antibacterial activities of lead compounds **6** and **34**. Given that *S. aureus* is the major cause of skin and soft tissue infection,[2,4] we established a murine skin infection model by subcutaneous injection of MRSA USA300-LAC, a clinically relevant and virulent strain. Treatment with compounds **6** and **34** significantly reduced the bacterial load on the skin (Figure 9c). Additionally, we also conducted a murine *S. aureus* bacteremia model due to the high risk for morbidity and mortality for *S. aureus* bacteremia. Treatment with compounds **6** and **34** successfully improved the survival rate of infected mice (Figure 9b). Although no statistically significant difference in bacterial load was observed in kidneys between the vehicle- and drug-treated groups (Figure S30), compounds **6** and **34** significantly reduced bacterial load in the lungs, liver, and heart (Figure 9d−f). These results highlight the in vivo efficacy of the synthetic cation transporters.

DISCUSSION

The disruption of ion homeostasis by synthetic ion transporters has previously been reported to inhibit bacterial growth, yet the development of these transporters as therapeutics has faced significant challenges, including their indiscriminate cytotoxicity and a lack of understanding of their modes of action.[12,13] Since bacteria and mammalian cells have distinct transmembrane ionic regulation and electric potential, selective antibacterial cation transporters can be developed by exploiting these fundamental electrochemical differences. In this study, we initially developed compound **6**, an α-aminoxy dipeptide that facilitates K^+/H^+ transport in liposomes and living *S. aureus*. Compound **6** exhibited inhibitory effects against a broad range of Gram-positive bacteria, including MRSA, with a suitable therapeutic window. Notably, compound **6** is the first synthetic cation transporter, to our knowledge, capable of eliminating the notoriously challenging *S. aureus* persisters. Compounds that can eradicate bacterial persisters are rare, with examples including synthetic retinoids,[63] acyldepsipeptides,[21] and human kinase inhibitors.[64] Furthermore, none of the FDA-approved antibiotics can eliminate persisters. It has been reported that PMF is essential for maintaining starvation-induced bacterial antibiotic tolerance in *E. coli*.[65] This further corroborates our finding that the disruption of PMF by synthetic cation transporters can effectively eliminate bacterial persisters. In addition to its activity against persisters, compound **6** demonstrated remarkable efficacy in eliminating biofilms composed of persisters. Considering that *S. aureus* biofilms significantly enhance antibiotic tolerance and worsen the prognosis of bacterial infections, our findings can potentially drive the development of new antibiofilm therapies targeting ion homeostasis. Optimization of compound **6** led to the discovery of compound **34**, which demonstrated enhanced antibacterial potency while maintaining a manageable toxicity profile. Given the simple synthetic route of cation transporters containing α-aminoxy amides, future work will focus on refining these structures to improve their pharmacological properties and broaden their antibacterial spectrum.

CONCLUSION

In conclusion, we have successfully developed a series of antibacterial cation transporters utilizing α-aminoxy acids as building blocks. By disrupting bacterial ion homeostasis, compounds **6** and **34** exhibited remarkable antibacterial activities, especially on *S. aureus* persisters and biofilm. Our results underscore the antibiotic potential of synthetic cation transporters as promising drug candidates for combating infections caused by antibiotic-resistant or persistent Gram-positive bacteria. We believe that the structural and biological insights from our study could pave the way for the development of new synthetic cation transporters, as well as other small molecules that could eradicate MDR bacteria and their persisters.

ASSOCIATED CONTENT

Supporting Information

The Supporting Information is available free of charge at https://pubs.acs.org/doi/10.1021/jacsau.4c01198.

General experimental procedures, supplementary figures and tables, chemical synthesis and characterization data of compounds **3**−**56**, and ^{1}H NMR, ^{13}C NMR, and ^{19}F NMR spectra of compounds **3**−**56** (PDF)

AUTHOR INFORMATION

Corresponding Authors

Richard Yi-Tsun Kao − *Department of Microbiology and Carol Yu Centre for Infection, The University of Hong Kong, Pokfulam, Hong Kong 999077, P. R. China*; Email: rytkao@hku.hk

Dan Yang − *Morningside Laboratory for Chemical Biology, Department of Chemistry, The University of Hong Kong, Pokfulam, Hong Kong 999077, P. R. China; School of Life Sciences, Westlake University, Hangzhou, Zhejiang 310024, China; Westlake Laboratory of Life Sciences and Biomedicine,*

https://doi.org/10.1021/jacsau.4c01198
JACS Au 2025, 5, 1328−1339

Hangzhou, Zhejiang 310024, China; orcid.org/0000-0002-1726-9335; Email: yangdan@westlake.edu.cn

Authors

Pak-Ming Fong − *Morningside Laboratory for Chemical Biology, Department of Chemistry, The University of Hong Kong, Pokfulam, Hong Kong 999077, P. R. China*

Victor Yat-Man Tang − *Department of Microbiology and Carol Yu Centre for Infection, The University of Hong Kong, Pokfulam, Hong Kong 999077, P. R. China*

Lu Xu − *School of Life Sciences, Westlake University, Hangzhou, Zhejiang 310024, China*

Bill Hin-Cheung Yam − *Department of Microbiology and Carol Yu Centre for Infection, The University of Hong Kong, Pokfulam, Hong Kong 999077, P. R. China*

Halebeedu Prakash Pradeep − *Department of Microbiology and Carol Yu Centre for Infection, The University of Hong Kong, Pokfulam, Hong Kong 999077, P. R. China*

Yuhui Feng − *School of Life Sciences, Westlake University, Hangzhou, Zhejiang 310024, China*

Liang Tao − *School of Life Sciences, Westlake University, Hangzhou, Zhejiang 310024, China; Westlake Laboratory of Life Sciences and Biomedicine, Hangzhou, Zhejiang 310024, China;* orcid.org/0000-0003-3441-698X

Complete contact information is available at: https://pubs.acs.org/10.1021/jacsau.4c01198

Author Contributions

All authors have approved the final version of the manuscript.

Notes

The authors declare no competing financial interest.

■ ACKNOWLEDGMENTS

This work was supported by The University of Hong Kong, Morningside Foundation, Westlake Education Foundation, and Hong Kong Research Grants Council under the Area of Excellence Scheme (AoE/P-705/16). We thank Prof. Shang Cai from Westlake University for providing primary human cells. We acknowledge the support from the Bioresearch Support Core of the Centre for PanorOmic Sciences (CPOS) of the Li Ka Shing Faculty of Medicine for the secretome and whole genome sequencing study, Electron Microscope Unit of The University of Hong Kong for the study using FESEM and TEM. We acknowledge financial support from the UGC-funded Support for Interdisciplinary Research in Chemical Science scheme administered by the HKU for electrospray ionization quadrupole time-of-flight mass spectrometry facilities. We thank Siu-Lun Bok for the proofreading of this manuscript.

■ REFERENCES

(1) Murray, C. J. L.; Ikuta, K. S.; Sharara, F.; Swetschinski, L.; Robles Aguilar, G.; Gray, A.; Han, C.; Bisignano, C.; Rao, P.; Wool, E.; et al. Global burden of bacterial antimicrobial resistance in 2019: a systematic analysis. *Lancet* **2022**, *399*, 629−655.

(2) Mork, R. L.; Hogan, P. G.; Muenks, C. E.; Boyle, M. G.; Thompson, R. M.; Sullivan, M. L.; Morelli, J. J.; Seigel, J.; Orscheln, R. C.; Bubeck Wardenburg, J.; Gehlert, S. J.; Burnham, C. D.; Rzhetsky, A.; Fritz, S. A. Longitudinal, strain-specific Staphylococcus aureus introduction and transmission events in households of children with community-associated meticillin-resistant S aureus skin and soft tissue infection: a prospective cohort study. *Lancet Infect. Dis.* **2020**, *20*, 188−198.

(3) Holland, T. L.; Arnold, C.; Fowler, V. G., Jr. Clinical management of Staphylococcus aureus bacteremia: a review. *JAMA* **2014**, *312*, 1330−1341.

(4) Lowy, F. D. Staphylococcus aureus infections. *N. Engl. J. Med.* **1998**, *339*, 520−532.

(5) Harms, A.; Maisonneuve, E.; Gerdes, K. Mechanisms of bacterial persistence during stress and antibiotic exposure. *Science* **2016**, *354*, aaf4268.

(6) Ciofu, O.; Moser, C.; Jensen, P. O.; Hoiby, N. Tolerance and resistance of microbial biofilms. *Nat. Rev. Microbiol.* **2022**, *20*, 621−635.

(7) Beyer, P.; Paulin, S. The antibacterial research and development pipeline needs urgent solutions. *ACS Infect. Dis.* **2020**, *6*, 1289−1291.

(8) Bremer, E.; Kramer, R. Responses of microorganisms to osmotic Stress. *Annu. Rev. Microbiol.* **2019**, *73*, 313−334.

(9) Kevin Ii, D. A.; Meujo, D. A. F.; Hamann, M. T. Polyether ionophores: broad-spectrum and promising biologically active molecules for the control of drug-resistant bacteria and parasites. *Expert Opin. Drug Discovery* **2009**, *4*, 109−146.

(10) Marques, R. D. S.; Cooke, R. F. Effects of ionophores on ruminal function of beef cattle. *Anim.* **2021**, *11*, 2871−2881.

(11) Aleman, M.; Magdesian, K. G.; Peterson, T. S.; Galey, F. D. Salinomycin toxicosis in horses. *J. Am. Vet. Med. Assoc.* **2007**, *230*, 1822−1826.

(12) Leevy, W. M.; Gammon, S. T.; Levchenko, T.; Daranciang, D. D.; Murillo, O.; Torchilin, V.; Piwnica-Worms, D.; Huettner, J. E.; Gokel, G. W. Structure-activity relationships, kinetics, selectivity, and mechanistic studies of synthetic hydraphile channels in bacterial and mammalian cells. *Org. Biomol. Chem.* **2005**, *3*, 3544−3550.

(13) Lin, S.; Liu, H.; Svenningsen, E. B.; Wollesen, M.; Jacobsen, K. M.; Andersen, F. D.; Moyano-Villameriel, J.; Pedersen, C. N.; Norby, P.; Torring, T.; Poulsen, T. B. Expanding the antibacterial selectivity of polyether ionophore antibiotics through diversity-focused semisynthesis. *Nat. Chem.* **2021**, *13*, 47−55.

(14) Shen, F. F.; Dai, S. Y.; Wong, N. K.; Deng, S.; Wong, A. S.; Yang, D. Mediating K^+/H^+ transport on organelle membranes to selectively eradicate cancer stem cells with a small molecule. *J. Am. Chem. Soc.* **2020**, *142*, 10769−10779.

(15) Zilberstein, D.; Agmon, V.; Schuldiner, S.; Padan, E. Escherichia coli intracellular pH, membrane potential, and cell growth. *J. Bacteriol.* **1984**, *158*, 246−252.

(16) Stock, U.; Matter, H.; Diekert, K.; Dorner, W.; Drose, S.; Licher, T. Measuring interference of drug-like molecules with the respiratory chain: toward the early identification of mitochondrial uncouplers in lead finding. *Assay Drug Dev. Technol.* **2013**, *11*, 408−422.

(17) Ruiz, N.; Falcone, B.; Kahne, D.; Silhavy, T. J. Chemical conditionality: a genetic strategy to probe organelle assembly. *Cell* **2005**, *121*, 307−317.

(18) Sampson, B. A.; Misra, R.; Benson, S. A. Identification and characterization of a new gene of Escherichia coli K-12 involved in outer membrane permeability. *Genetics* **1989**, *122*, 491−501.

(19) Rasko, D.; Sperandio, V. Anti-virulence strategies to combat bacteria-mediated disease. *Nat. Rev. Drug Discovery* **2010**, *9*, 117−128.

(20) Foster, T. Immune evasion by staphylococci. *Nat. Rev. Microbiol.* **2005**, *3*, 948−958.

(21) Conlon, B. P.; Nakayasu, E. S.; Fleck, L. E.; LaFleur, M. D.; Isabella, V. M.; Coleman, K.; Leonard, S. N.; Smith, R. D.; Adkins, J. N.; Lewis, K. Activated ClpP kills persisters and eradicates a chronic biofilm infection. *Nature* **2013**, *503*, 365−370.

(22) Stewart, P. S. Mechanisms of antibiotic resistance in bacterial biofilms. *Int. J. Med. Microbiol.* **2002**, *292*, 107−113.

(23) Spooner, M. J.; Li, H.; Marques, I.; Costa, P. M. R.; Wu, X.; Howe, E. N. W.; Busschaert, N.; Moore, S. J.; Light, M. E.; Sheppard, D. N.; Félix, V.; Gale, P. A. Fluorinated synthetic anion carriers: experimental and computational insights into transmembrane chloride transport. *Chem. Sci.* **2019**, *10*, 1976−1985.

(24) Wu, X.; Judd, L. W.; Howe, E. N. W.; Withecombe, A. M.; Soto-Cerrato, V.; Li, H.; Busschaert, N.; Valkenier, H.; Pérez-Tomás, R.; Sheppard, D. N.; Jiang, Y.-B.; Davis, A. P.; Gale, P. A. Non-

protonophoric electrogenic Cl^- transport mediated by valinomycin-like carriers. *Chem* **2016**, *1*, 127−146.
(25) Li, X.; Shen, B.; Yao, X. Q.; Yang, D. A. Small synthetic molecule forms chloride channels to mediate chloride transport across cell membranes. *J. Am. Chem. Soc.* **2007**, *129*, 7264−7265.
(26) Maloney, P. C.; Kashket, E. R.; Wilson, T. H. A protonmotive force drives ATP synthesis in bacteria. *Proc. Natl. Acad. Sci. U.S.A.* **1974**, *71*, 3896−3900.
(27) Iu, H.-T.-V.; Fong, P.-M.; Yam, H.-C.-B.; Gao, P.; Yan, B.; Lai, P.-M.; Tang, V.-Y.-M.; Li, K.-H.; Ma, C.-W.; Ng, K.-H.-K.; Sze, K. H.; Yang, D.; Davies, J.; Kao, R. Y. Identification of a small molecule compound active against antibiotic-tolerant Staphylococcus aureus by boosting ATP synthesis. *Int. J. Mol. Sci.* **2023**, *24*, 6242.
(28) Tharmalingam, N.; Jayamani, E.; Rajamuthiah, R.; Castillo, D.; Fuchs, B. B.; Kelso, M. J.; Mylonakis, E. Activity of a novel protonophore against methicillin-resistant Staphylococcus aureus. *Future Med. Chem.* **2017**, *9*, 1401−1411.
(29) Silverman, J. A.; Perlmutter, N. G.; Shapiro, H. M. Correlation of daptomycin bactericidal activity and membrane depolarization in Staphylococcus aureus. *Antimicrob. Agents Chemother.* **2003**, *47*, 2538−2544.
(30) Farha, M. A.; Verschoor, C. P.; Bowdish, D.; Brown, E. D. Collapsing the proton motive force to identify synergistic combinations against Staphylococcus aureus. *Chem. Biol.* **2013**, *20*, 1168−1178.
(31) Allison, K. R.; Brynildsen, M. P.; Collins, J. J. Metabolite-enabled eradication of bacterial persisters by aminoglycosides. *Nature* **2011**, *473*, 216−220.
(32) Armstrong, C. M.; Hille, B. Voltage-gated ion channels and electrical excitability. *Neuron* **1998**, *20*, 371−380.
(33) Berridge, M. J. Neuronal calcium signaling. *Neuron* **1998**, *21*, 13−26.
(34) Cho, C. H.; Woo, J. S.; Perez, C. F.; Lee, E. H. A focus on extracellular Ca^{2+} entry into skeletal muscle. *Exp. Mol. Med.* **2017**, *49*, No. e378.
(35) Rizzuto, R.; Pinton, P.; Ferrari, D.; Chami, M.; Szabadkai, G.; Magalhães, P. J.; Virgilio, F. D.; Pozzan, T. Calcium and apoptosis: facts and hypotheses. *Oncogene* **2003**, *22*, 8619−8627.
(36) Clementi, E. A.; Marks, L. R.; Duffey, M. E.; Hakansson, A. P. A novel initiation mechanism of death in Streptococcus pneumoniae induced by the human milk protein-lipid complex HAMLET and activated during physiological death. *J. Biol. Chem.* **2012**, *287*, 27168−27182.
(37) Yu, X.; Duan, K. L.; Shang, C. F.; Yu, H. G.; Zhou, Z. Calcium influx through hyperpolarization-activated cation channels (I(h) channels) contributes to activity-evoked neuronal secretion. *Proc. Natl. Acad. Sci. U.S.A.* **2004**, *101*, 1051−1056.
(38) Li, X.; Shen, B.; Yao, X. Q.; Yang, D. Synthetic chloride channel regulates cell membrane potentials and voltage-gated calcium channels. *J. Am. Chem. Soc.* **2009**, *131*, 13676−13680.
(39) Lee, K. S.; Tsien, R. W. Mechanism of calcium channel blockade by verapamil, D600, diltiazem and nitrendipine in single dialysed heart cells. *Nature* **1983**, *302*, 790−794.
(40) Kitakaze, M.; Karasawa, A.; Kobayashi, H.; Tanaka, H.; Kuzuya, T.; Hori, M. Benidipine: A new Ca^{2+} channel blocker with a cardioprotective effect. *Cardiovasc. Drug Rev.* **1999**, *17*, 1−15.
(41) Tarasov, A. I.; Griffiths, E. J.; Rutter, G. A. Regulation of ATP production by mitochondrial Ca^{2+}. *Cell Calcium* **2012**, *52*, 28−35.
(42) Brookes, P. S.; Yoon, Y.; Robotham, J. L.; Anders, M. W.; Sheu, S. S. Calcium, ATP, and ROS: a mitochondrial love-hate triangle. *Am. J. Physiol.* **2004**, *287*, C817−C833.
(43) Bruni, G. N.; Kralj, J. M. Membrane voltage dysregulation driven by metabolic dysfunction underlies bactericidal activity of aminoglycosides. *Elife* **2020**, *9*, No. e58706.
(44) Imai, Y.; Meyer, K. J.; Iinishi, A.; Favre-Godal, Q.; Green, R.; Manuse, S.; Caboni, M.; Mori, M.; Niles, S.; Ghiglieri, M.; Honrao, C.; Ma, X.; Guo, J. J.; Makriyannis, A.; Linares-Otoya, L.; Böhringer, N.; Wuisan, Z. G.; Kaur, H.; Wu, R.; Mateus, A.; Typas, A.; Savitski, M. M.; Espinoza, J. L.; O'Rourke, A.; Nelson, K. E.; Hiller, S.; Noinaj, N.; Schäberle, T. F.; D'Onofrio, A.; Lewis, K. A new antibiotic selectively kills Gram-negative pathogens. *Nature* **2019**, *576*, 459−464.
(45) Chan, Y. G.; Frankel, M. B.; Missiakas, D.; Schneewind, O. SagB glucosaminidase is a determinant of Staphylococcus aureus glycan chain length, antibiotic susceptibility, and protein secretion. *J. Bacteriol.* **2016**, *198*, 1123−1136.
(46) Schaefer, K.; Owens, T. W.; Page, J. E.; Santiago, M.; Kahne, D.; Walker, S. Structure and reconstitution of a hydrolase complex that may release peptidoglycan from the membrane after polymerization. *Nat. Microbiol.* **2021**, *6*, 34−43.
(47) Dubrac, S.; Boneca, I. G.; Poupel, O.; Msadek, T. New insights into the WalK/WalR (YycG/YycF) essential signal transduction pathway reveal a major role in controlling cell wall metabolism and biofilm formation in Staphylococcus aureus. *J. Bacteriol.* **2007**, *189*, 8257−8269.
(48) Gajdiss, M.; Monk, I. R.; Bertsche, U.; Kienemund, J.; Funk, T.; Dietrich, A.; Hort, M.; Sib, E.; Stinear, T. P.; Bierbaum, G. YycH and YycI regulate expression of Staphylococcus aureus autolysins by activation of WalRK phosphorylation. *Microorganisms* **2020**, *8*, 870.
(49) Dobihal, G. S.; Brunet, Y. R.; Flores-Kim, J.; Rudner, D. Z. Homeostatic control of cell wall hydrolysis by the WalRK two-component signaling pathway in Bacillus subtilis. *eLife* **2019**, *8*, No. e52088.
(50) Fournier, B.; Hooper, D. C. A new two-component regulatory system involved in adhesion, autolysis, and extracellular proteolytic activity of Staphylococcus aureus. *J. Bacteriol.* **2000**, *182*, 3955−3964.
(51) Bose, J. L.; Lehman, M. K.; Fey, P. D.; Bayles, K. W. Contribution of the Staphylococcus aureus Atl AM and GL murein hydrolase activities in cell division, autolysis, and biofilm formation. *PloS One* **2012**, *7* (7), No. e42244.
(52) Pinho, M. G.; Kjos, M.; Veening, J. W. How to get (a)round: mechanisms controlling growth and division of coccoid bacteria. *Nat. Rev. Microbiol.* **2013**, *11*, 601−614.
(53) Antignac, A.; Sieradzki, K.; Tomasz, A. Perturbation of cell wall synthesis suppresses autolysis in Staphylococcus aureus: evidence for coregulation of cell wall synthetic and hydrolytic enzymes. *J. Bacteriol.* **2007**, *189*, 7573−7580.
(54) Dobihal, G. S.; Flores-Kim, J.; Roney, I. J.; Wang, X.; Rudner, D. Z. The WalR-WalK signaling pathway modulates the activities of both CwlO and LytE through control of the peptidoglycan deacetylase PdaC in Bacillus subtilis. *J. Bacteriol.* **2022**, *204*, 005333.
(55) Rice, K.; Peralta, R.; Bast, D.; de Azavedo, J.; McGavin, M. J. Description of staphylococcus serine protease (ssp) operon in Staphylococcus aureus and nonpolar inactivation of sspA-encoded serine protease. *Infect. Immun.* **2001**, *69*, 159−169.
(56) Madiraju, M. V.; Brunner, D. P.; Wilkinson, B. J. Effects of temperature, NaCl, and methicillin on penicillin-binding proteins, growth, peptidoglycan synthesis, and autolysis in methicillin-resistant Staphylococcus aureus. *Antimicrob. Agents Chemother.* **1987**, *31*, 1727−1733.
(57) Kemper, M. A.; Urrutia, M. M.; Beveridge, T. J.; Koch, A. L.; Doyle, R. J. Proton motive force may regulate cell wall-associated enzymes of Bacillus subtilis. *J. Bacteriol.* **1993**, *175*, 5690−5696.
(58) Jolliffe, L. K.; Doyle, R. J.; Streips, U. N. The energized membrane and cellular autolysis in Bacillus subtilis. *Cell* **1981**, *25*, 753−763.
(59) Lutzner, N.; Patzold, B.; Zoll, S.; Stehle, T.; Kalbacher, H. Development of a novel fluorescent substrate for Autolysin E, a bacterial type II amidase. *Biochem. Biophys. Res. Commun.* **2009**, *380*, 554−558.
(60) Eckert, C.; Lecerf, M.; Dubost, L.; Arthur, M.; Mesnage, S. Functional analysis of AtlA, the major N-acetylglucosaminidase of Enterococcus faecalis. *J. Bacteriol.* **2006**, *188*, 8513−8519.
(61) Calamita, H. G.; Ehringer, W. D.; Koch, A. L.; Doyle, R. J. Evidence that the cell wall of Bacillus subtilis is protonated during respiration. *Proc. Natl. Acad. Sci. U S A* **2001**, *98*, 15260−15263.
(62) Biswas, R.; Martinez, R. E.; Gohring, N.; Schlag, M.; Josten, M.; Xia, G.; Hegler, F.; Gekeler, C.; Gleske, A. K.; Gotz, F.; Sahl, H. G.; Kappler, A.; Peschel, A. Proton-binding capacity of Staphylococcus

https://doi.org/10.1021/jacsau.4c01198
JACS Au 2025, 5, 1328−1339

aureus wall teichoic acid and its role in controlling autolysin activity. *PLoS One* **2012**, *7*, No. e41415.
(63) Kim, W.; Zhu, W.; Hendricks, G. L.; Van Tyne, D.; Steele, A. D.; Keohane, C. E.; Fricke, N.; Conery, A. L.; Shen, S.; Pan, W.; Lee, K.; Rajamuthiah, R.; Fuchs, B. B.; Vlahovska, P. M.; Wuest, W. M.; Gilmore, M. S.; Gao, H.; Ausubel, F. M.; Mylonakis, E. A new class of synthetic retinoid antibiotics effective against bacterial persisters. *Nature* **2018**, *556*, 103−107.
(64) Le, P.; Kunold, E.; Macsics, R.; Rox, K.; Jennings, M. C.; Ugur, I.; Reinecke, M.; Chaves-Moreno, D.; Hackl, M. W.; Fetzer, C.; Mandl, F. A. M.; Lehmann, J.; Korotkov, V. S.; Hacker, S. M.; Kuster, B.; Antes, I.; Pieper, D. H.; Rohde, M.; Wuest, W. M.; Medina, E.; Sieber, S. A. Repurposing human kinase inhibitors to create an antibiotic active against drug-resistant Staphylococcus aureus, persisters and biofilms. *Nat. Chem.* **2020**, *12*, 145−158.
(65) Wang, M.; Chan, E. W. C.; Wan, Y.; Wong, M. H.; Chen, S. Active maintenance of proton motive force mediates starvation-induced bacterial antibiotic tolerance in Escherichia coli. *Commun. Biol.* **2021**, *4*, 1068.

https://doi.org/10.1021/jacsau.4c01198
JACS Au 2025, 5, 1328−1339